Vibrationally state-selected reactions of ammonia ions. I. $NH_3^+(v) + D_2$

Richard J. S. Morrison,[a] William E. Conaway, Takayuki Ebata, and Richard N. Zare
Department of Chemistry, Stanford University, Stanford, California 94305

(Received 14 January 1986; accepted 11 February 1986)

Resonance enhanced multiphoton ionization has been applied to the production of vibrationally state-selected ion beams. Ammonia ions are selectively formed with a specific number of vibrational quanta in the ν_2 umbrella bending mode. The effect of vibrational excitation of this mode on the reaction of NH_3^+ ($\tilde{X}$, $v = 0$ to 9) with D_2 is examined over the 0.5 to 10 eV center-of-mass kinetic energy range in a tandem quadrupole mass spectrometer. Under these conditions, (1) abstraction of a D atom to form NH_3D^+ is the dominant reaction channel, (2) NH_3D^+ having sufficient internal energy may decompose to yield NH_2D^+ and this decomposition process is enhanced by vibrational excitation of the NH_3^+ reagent, and (3) NH_2D^+ is also formed by direct hydrogen–deuterium exchange of NH_3^+ with D_2, but this channel appears as a minor contribution which is insensitive to the vibrational excitation of the NH_3^+. A spectator stripping model is able to account for the ratio of NH_2D^+ to NH_3D^+ as a function of the NH_3^+ translational and vibrational energy.

I. INTRODUCTION

In the field of ion–molecule reaction dynamics, state-resolved studies were first pioneered by Chupka, Russell, and Rafaey,[1] who examined the vibrational dependence of the reaction $H_2^+(v) + H_2 \rightarrow H_3^+ + H$. The H_2^+ ions were produced in selected vibrational levels by direct one-photon vacuum ultraviolet (VUV) photoionization of H_2. The relative yields of H_2^+ and H_3^+ as a function of the ionization wavelength were compared to give the vibrational dependence of the reaction cross section. The VUV photoionization technique is still in extensive use.[2] A second technique for selecting ions in specific vibrational states is that of photoion–photoelectron coincidence developed by Baer and co-workers[3] and by Tanaka and Koyano.[4] The sample gas is photoionized by a vacuum ultraviolet lamp or by synchrotron radiation. The ejected photoelectrons and the photoions, after drifting through the neutral reactant gas, are then detected in coincidence to determine the internal energy state of the ions. Bowers and co-workers[5] have used selective charge transfer reactions to produce ions of varying internal energy for reactive studies in a tandem ICR mass spectrometer. Ions such as CO_2^+, Xe^+, Kr^+, and Ar^+ are formed by electron impact and allowed to charge transfer with the neutral sample. This leaves the ionized sample molecule with a characterizable amount of internal excitation before reaction. The flowing afterglow technique used by Ferguson *et al.*[6] has also made important contributions to the study of vibrational effects on ion–neutral reactions.

The approach used in the present study is to prepare reagent ions in a quantum-state-specific manner using resonance enhanced multiphoton ionization (MPI).[7] This technique takes advantage of the high similarity between the structure of the resonant intermediate Rydberg state and the structure of the ion ground state. Direct ionization from a vibrational level in the Rydberg state follows the Franck–Condon principle and hence predominantly favors the transition to the same vibrational level in the ion.[8–10] The ion vibrational level is selected simply by tuning the laser frequency to be resonant with the same vibrational level of the Rydberg intermediate state. Thus, it is possible to use $n + 1$ MPI to produce high densities of pure, vibrationally state-selected ions for reaction dynamics studies.

Ammonia is an ideal candidate for state-selective ionization by this method and, in addition, possesses rich ion chemistry. Because reactions to form NH_4^+ are important in many chemical systems, the reactions of NH_3^+ and H_2/D_2 have been of interest. The earliest studies on this system were performed on mixtures of NH_3 and D_2 in the ionization regions of mass spectrometers and the reaction was found to be extremely inefficient.[11,12] The beam-gas study by Eisele *et al.*[13] detected both the exothermic deuterium abstraction product and the thermoneutral hydrogen–deuterium exchange product:

$$NH_3^+ + D_2 \rightarrow NH_3D^+ + D, \quad \Delta H = -1.04\ \text{eV}, \quad (1)$$

$$NH_3^+ + D_2 \rightarrow NH_2D^+ + HD, \quad \Delta H = -0.02\ \text{eV}. \quad (2)$$

No indication of isotopic scrambling was found suggesting that the $NH_3^+ + D_2$ reaction does not proceed through a long-lived complex at the center-of-mass energies examined (0.5–10 eV). The angular distribution of the products indicates that the reaction is strongly forward scattered, providing additional evidence that the reaction proceeds by a direct mechanism. The observed increase in NH_2D^+ at kinetic energies above 4 eV in the center-of-mass (c.m.) was attributed to the opening of a new channel for NH_2D^+ formation:

$$NH_3^+ + D_2 \rightarrow [NH_3D^+]^* + D \begin{cases} \nearrow NH_2D^+ + H + D \\ \searrow NH_3^+ + D + D \end{cases} \quad (3)$$

Additional evidence suggested the existence of an early barrier in the abstraction channel which was attributed to the repulsion of the D_2 by the hydrogen atoms on the NH_3^+.

[a] Present address: Chemistry Department, Monash University, Clayton, Victoria 3168, Australia.

 0021-9606/86/105527-09$02.10

The ICR study of Kim, Theard, and Huntress[14] and the flowing afterglow study of Fehsenfeld *et al.*[15] have established the near-thermal abstraction rate coefficient to be $\leqslant 5\times 10^{-13}\,\mathrm{cm^3\,s^{-1}}$ and to depend strongly on the ion kinetic energy. A 90 meV barrier was also postulated to occur early in the abstraction channel based on this strong kinetic energy dependence.[15] Low temperature studies by Smith and Adams[16] using a selected ion flow tube and by Luine[17] and Barlow[18] in Dunn's laboratory using a He cooled ion trap indicate that complex formation and quantum mechanical tunneling become important at very low temperatures.

The effect of vibrational excitation of the H_2/D_2 on the abstraction channel has been noted by Fehsenfeld and coworkers[15] to increase the reaction efficiency. Photoionization studies by Karachevtsev *et al.*[19] suggest that the reaction cross section increases with vibrational excitation of the NH_3^+, but the authors fail to mention the appearance of the exchange channel. Most recently, Kemper and Bowers[20] have examined the kinetic energy dependence (0–1 eV) and internal energy dependence (1–5 eV) of these reactions in a series of tandem ICR experiments using selective charge transfer reactions. They concluded that the formation of NH_2D^+ is driven predominantly by vibrational energy whereas the formation of NH_3D^+ is driven predominantly by kinetic energy. Complex formation was found to be important only below 100 K.

The present tandem quadrupole study investigates the effect on reactions (1)–(3) of varying the kinetic energy of the NH_3^+ ion from 0.5 to 10 eV in the center-of-mass and the vibrational excitation of the ν_2 umbrella-bending mode from 0–1.1 eV ($v=0$ to $v=9$). The results are compared with other experiments and with simple theoretical models.

II. EXPERIMENTAL TECHNIQUES

A. Overview

Figure 1 shows a schematic diagram of the experimental apparatus. The apparatus was described briefly in a previous publication,[7] and several major improvements have been incorporated into the system since that time. The first improvement has been the addition of a quadrupole mass filter in front of the reaction cell to provide mass selection of the primary ion beam. The second has been a change in the method by which the kinetic energy of the primary ions is varied. These improvements have helped to reduce the background signal at the product ion masses and to improve the product ion collection efficiency.

The current system is operated as a tandem quadrupole mass spectrometer with a pulsed laser ionization source. The state-selected ions formed by the laser are first collimated into a beam, mass selected, and then focused at controlled kinetic energy into a field-free static gas cell containing the neutral reactant partner. The secondary ions formed as products of the reaction are collected, mass analyzed, and detected. The effect of the initial primary ion quantum state on the individual product ion channels can be examined at various kinetic energies.

The system in principle is similar to conventional tandem mass spectrometers used in the study of ion–molecule reactions in that it provides a mass-selected reactant ion beam and mass analysis of the product ions.[21] However, rather than create the ions by electron impact ionization or by chemical ionization, which produce distributions over the various possible ion states, the ions are formed in a highly specific, vibrationally state-selective fashion by laser multiphoton ionization. The initial state selection will remain intact if the ions react before collisional or radiative relaxation can occur. In addition, weak coupling of the excited mode to the other vibrational modes in the ion limits randomization of the energy for small polyatomic ions.

B. Vibrational state selection of ammonia ions

The $\tilde{B}$ and $\tilde{C}'$ electronic states of ammonia have been studied quite extensively by 3 + 1 and 2 + 1 multiphoton ionization.[22–28] The ν_2 umbrella-bending mode vibration connects the planar geometry of the Rydberg states with the pyramidal geometry of the ground state. As shown in Fig. 2, a long progression in this vibrational mode (960 $\mathrm{cm^{-1}}$, 120 meV) dominates the spectrum of the $\tilde{B}$ and $\tilde{C}'$ states. Although these two states overlap, sufficient cooling of the sample in a supersonic expansion allows the spectra to be resolved cleanly. Cooling also concentrates population in the lowest rotational levels. Calculation of the Franck–Condon overlap between these Rydberg states and the ion ground state indicates that the transitions are nearly diagonal. Thus, it is predicted that direct ionization will produce the same vibrational level in the ion as the resonant vibrational level in

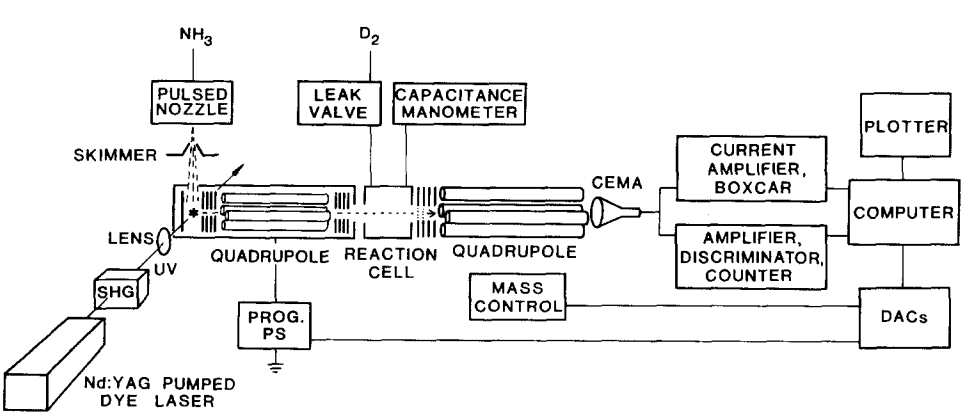

FIG. 1. Schematic diagram of the tandem quadrupole mass spectrometer with laser multiphoton ionization source.

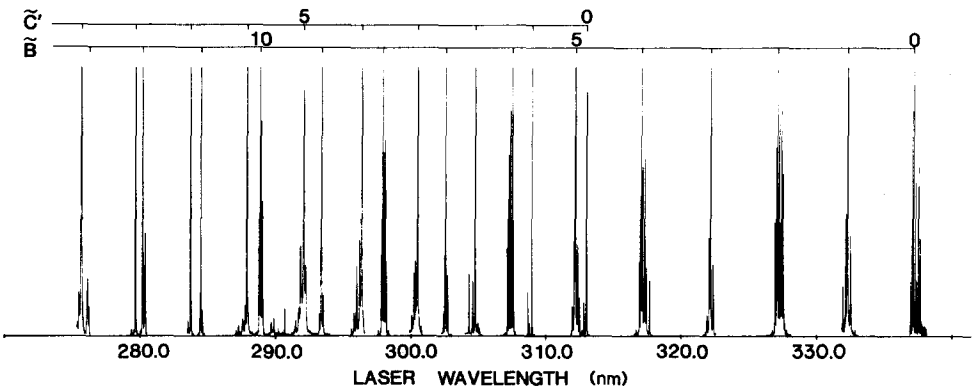

FIG. 2. 2 + 1 MPI spectrum of the ammonia $\tilde{B}$ and $\tilde{C}'$ states in the 275–345 nm range showing the interleaved progression in the ν_2 bending mode. Individual vibrational bands have not been normalized to constant laser power. The rotational temperature is 12–15 K.

the Rydberg state. This has been confirmed experimentally by examining the kinetic energy distribution of the photoelectrons produced in the ionization step.[28] As shown in Fig. 3, photoelectrons produced by the $\Delta v = 0$ transition are the single dominant feature in the MPI-photoelectron spectra of both the $\tilde{B}$ and $\tilde{C}'$ states.

The $\tilde{C}'$ state has been used exclusively in this study due to its simpler MPI spectrum and high efficiency of the $\Delta v = 0$ transition, as seen from its MPI-photoelectron spectra. Due to the high laser power densities used in the experiment to maximize the ion yield, it has been found that subsequent absorption of additional photons by the ammonia ions leads to a measurable amount of fragmentation.[7,23] This situation is further complicated in studies where ND_3 is used and accidental overlaps with the $^{14}NH_2D$, $^{14}NHD_2$, $^{14}NH_3$, and analogous ^{15}N isotopic resonances cause additional mass contamination of the ion beam. Consequently, a quadrupole mass filter is used to mass select the ion beam before reaction.

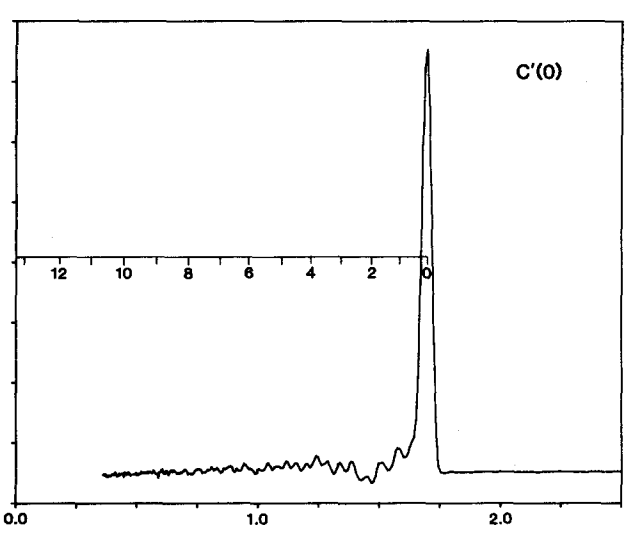

FIG. 3. Photoelectron kinetic energy distribution produced by 2 + 1 MPI resonant with the $v = 0$ level of the $\tilde{C}'$ state. The horizontal ladder indicates the corresponding vibrational levels of the ion ground state.

C. Vacuum system

The vacuum system is divided into three major regions: (1) the differentially pumped molecular beam source, (2) the ionization chamber, and (3) the reaction/detection chamber. With the pulsed nozzle operating at 10 Hz and 20 psia backing pressure, the nozzle and differential chamber pressures are $\sim 5\times10^{-6}$ Torr ($\sim 7\times10^{-4}$ Pa) and $\sim 1\times10^{-7}$ Torr ($\sim 1\times10^{-5}$ Pa), respectively. The ionization chamber permits the laser to be focused onto the molecular beam and houses the primary ion beam quadrupole mass filter. The pressure in this chamber is $\sim 5\times10^{-8}$ Torr with the molecular beam source operational. The reaction chamber contains the reaction cell and the detection quadrupole mass filter. With a continuous gas flow to maintain the reaction cell pressure at 1.0 mTorr, the chamber pressure is $\sim 5\times10^{-6}$ Torr. The chamber itself is mounted on linear rails which allows easy access to both the pulsed nozzle source and to the ion optics system.

D. Ion source

The ion source is composed of three major components: (1) the molecular beam source, (2) the photon source, and (3) the mass-selection quadrupole. A commercial pulsed nozzle (Lasertechnics LPV-1) with a 0.1 mm orifice is used to provide a supersonic expansion of a 1:10 ammonia–argon mixture. Typical pulse durations are 100–150 μs. The expansion is skimmed (Beam Dynamics skimmer) and collimated before it enters the ionization region. The rotational temperature of the ammonia at the laser focus was determined to be 12–15 K from its 2 + 1 MPI spectrum. The *ortho* and *para* forms of ammonia have slightly different rotational temperatures since they relax at different rates in the expansion, as pointed out by Raymond and Kay.[29]

The ionizing laser radiation is provided by the frequency-doubled output of a 10 Hz Nd:YAG-pumped dye laser system (Quanta Ray DCR-1A, Quanta Ray PDL-1). Ultraviolet output over the range 275–315 nm covers the ν_2 $v = 0$ to $v = 9$ levels of the $\tilde{C}'$ Rydberg state. Within each level, the frequency was adjusted to the intense Q branch rotational line. Typical pulse energies ranged from 0.5 to 3.0 mJ, depending on the vibrational level. This results in the production of an estimated 10^5 state-selected ammonia ions per shot.

The laser is brought to a focus by a 250 mm lens between a pair of repeller and extractor plates, 9.2 cm downstream of the nozzle. The ions are drawn out of the ionization volume at a right angle to the molecular beam by a 5 V cm^{-1} electric field and pass through an aperture in the extractor. A small field is also applied transverse to the molecular beam to cancel the initial velocity component of the ion resulting from the translation of its neutral precursor. A symmetric einzel lens is used to focus the ion packet into the mass-selection quadrupole (Finnegan Series 3000) operated in a fixed mass mode. After exiting the quadrupole, the ions are refocused by another symmetric einzel lens and accelerated into the reaction chamber.

E. Reaction cell

Before entering the reaction cell, the ions are decelerated by a periodic focusing potential applied to a system of seven cylindrical ion lenses. The stainless steel reaction cell is 1.5 cm long and is located ~ 50 cm from the laser focus. Entrance aperture and exit aperture serve to define the physical extent of the cell and to maintain a pressure differential with respect to the remainder of the reaction chamber. Reactant gas is admitted to the cell through a gas port and the flow is regulated by a leak valve (Granville Phillips Series 216). The cell pressure is monitored by a capacitance manometer (MKS Baratron Type 220-BHS) and can be used to control the leak valve to maintain a set pressure. The precision of the capacitance manometer pressure measurement is 0.1 mTorr (0.013 Pa). A cell pressure of 1.0 mTorr (0.13 Pa) was chosen which results in a 10% attenuation of the primary ion signal. This insures that reactions are occurring under single-collision conditions and that only $\sim 1\%$ of the ions are undergoing multiple collisions. The mean free path of the deuterium at this pressure is 8 cm.

Reactions in the cell occur under field-free conditions. A product ion must be forward scattered in the laboratory reference frame with sufficient velocity to pass through the exit aperture to be collected by the quadrupole. The kinematics of a heavy + light $\rightarrow$ heavy–light system permits nearly all of the product ions to be strongly forward scattered out of the cell. However, for isotropically scattered product ions (in the lab reference frame), the ratio of the cell length to the exit aperture diameter determines the fraction of ions that will escape the reaction cell. With the cell dimensions given above, it is calculated that roughly 10% of these ions would be collected.

F. Product ion detection

Product ions and unreacted primary ions are focused by an asymmetric einzel lens into the mass-analysis quadrupole (Extranuclear Laboratories #4-270-9 with Model 12 High-Q Head) operated under external computer control. The ions are detected by a channel electron multiplier array (Galileo Electronics FTD-2002) at a gain of 10^7. Product ion pulses are amplified (EG&G Ortec 574) and fed into a 100 MHz discriminator (EG&G Ortec model 436) and accumulated by a 20 MHz gated counter (EG&G Ortec model 776). The intense primary ion signal, which would overrun the discriminator/counter, is instead fed into a current amplifier (Keithley model 427) and boxcar integrator (Princeton Applied Research 162/164).

G. Computer control

A Z-80 based miniprocessor (Altos Computer Systems) is used for controlling the experiment as well as for performing the data collection and analysis. The kinetic energy of the primary ion beam through the reaction cell corresponds to the difference in potential between the ion region and the reaction cell. By applying a dc offset voltage via a programmable power supply (Kepco BOP model 36-5M) to the entire ion-optics system upto the reaction cell, the kinetic energy of the ion through the cell can be scanned by the computer from 1 to 50 eV in the laboratory reference frame.

For each vibrational level, the system is set up to scan through the ion energy while recording the ion counts at each product mass. Due to the pulsed nature of the experiment, only one mass can be collected on each shot. A scan consists of stepping the ion energy and reading each product ion count after a set number of laser shots. The intensity of the primary ion beam is measured at the beginning of each scan to provide the means for normalizing the runs. This process is repeated ten or more times and a typical run lasts 2 h.

H. Ion energy calibration and energy spread

The actual laboratory ion energy can differ by several eV from that estimated from the potentials in the ionization region. It is therefore necessary to calibrate the offset by measuring the ion time of flight through a fixed pathlength as a function of the potential in that region. A nonlinear least squares curve fit of the flight times gives the actual zero of energy in the laboratory reference frame with an uncertainty of ± 0.5 eV. The primary ion flight time to the reaction cell is $\sim 25\ \mu s$ and, depending on the ion energy, the flight time to the detector is 40 to 50 μs. The spread in the laboratory energy was estimated to be at most 1 eV using the retarding field technique. Since this is much greater than the estimated spread from the finite extent of the laser focus in the ion source, this is attributed to the spread acquired in the quadrupole mass filter.

All energies are reported in the center of mass reference frame of the reagents. The kinetic energy in the center-of-mass, $E_{c.m.}$, is related to the laboratory kinetic energy, E_{lab}, by

$$E_{c.m.} = E_{lab} m_2/(m_1 + m_2), \tag{4}$$

where m_1 is the ion mass and m_2 is the target molecule mass. This assumes that the velocity of the thermal target molecule is negligible with respect to the velocity of the ion. The lab energy to center-of-mass energy conversion factor for the $NH_3^+ + D_2$ system is 0.19. Hence, there is at most a 0.2 eV energy spread in the center-of-mass frame for this particular reaction system.

The collection efficiency and resolution of the final quadrupole mass filter both depend on the energy of the product ions. This has two subtle consequences: (1) The product ion signal is further dependent on the kinetic energy of the pri-

mary ions, and (2) the various product mass channels may be detected preferentially if the associated kinetic energy release of the channels differ. For these reasons, the data are presented in terms of relative ion intensity rather than as an absolute cross section, which many other experiments are better suited to measure.

III. RESULTS

The mass spectrum in Fig. 4 shows the product masses observed for the reaction of NH_3^+ with D_2. The peak at mass 19 is assigned to the abstraction product, NH_3D^+ [reaction (1)]. The peak at mass 18 is assigned to the exchange product, NH_2D^+ [reactions (2) and (3)]. Although other isotope combinations are possible at these masses if one considers a scrambling mechanism to be operative, experiments performed with this apparatus on $ND_3^+ + H_2$ confirm that these assignments are correct and indeed unambiguous. No other products at higher or lower mass are observed. Despite the inefficiency of this reaction, count rates on the order of 1–2 counts per shot are measured at high kinetic energies.

The dependence of the product ion peak intensities with kinetic energy are shown in Fig. 5 for three different initial vibrational excitations of the ammonia ion. The data have been normalized to constant primary ion flux across the kinetic energy range and from vibrational level to vibrational level. The NH_3D^+ channel increases monotonically with kinetic energy upto 4–5 eV, where it levels off and begins to fall. The NH_2D^+ product is very weak at low NH_3^+ kinetic energy, but increases dramatically at higher kinetic energy. The onset and magnitude of this increase correspond directly with the decrease observed for the NH_3D^+ product ion.

Vibrational excitation appears to have little effect on either channel below 4–5 eV. Above this energy, increasing the vibrational level of the incident NH_3^+ ion tends to decrease the NH_3D^+ product ion intensity at any given energy and increase the NH_2D^+ product ion intensity, suggesting that the two product channels are not independent of one another. The variation of the signals with v is smooth and there is no evidence of any resonance effect. Vibration does not affect the *total* product ion yield within the experimental uncertainty of $\pm$ 10%.

The data is simplified by plotting the branching ratio

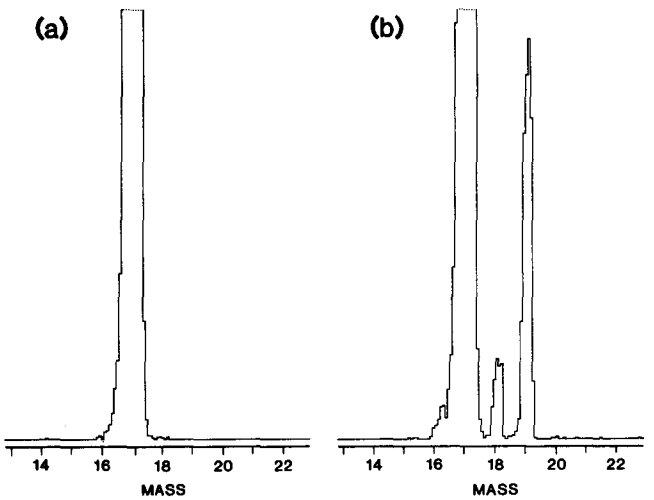

FIG. 4. Mass spectrum with 5 eV c.m. NH_3^+ ions: (a) without reactant gas, and (b) with 1.0 mTorr of D_2 present. The unreacted NH_3^+ appears at mass 17, NH_2D^+ appears at mass 18, and NH_3D^+ appears at mass 19.

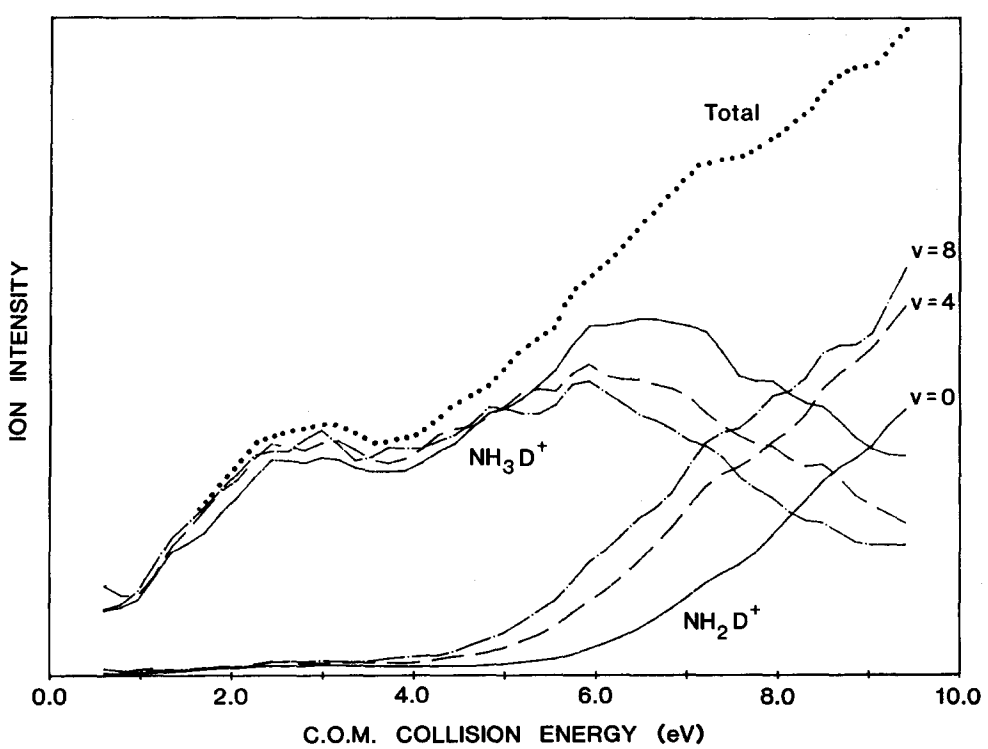

FIG. 5. Kinetic energy dependence of the product ion signals for three different NH_3^+ (v) vibrational levels. The dotted line is the total product ion yield, including the estimated NH_3^+ product. The total ion yield is independent of v within the experimental uncertainty of 10% which arises from the normalization of the primary ion signal at each laser frequency.

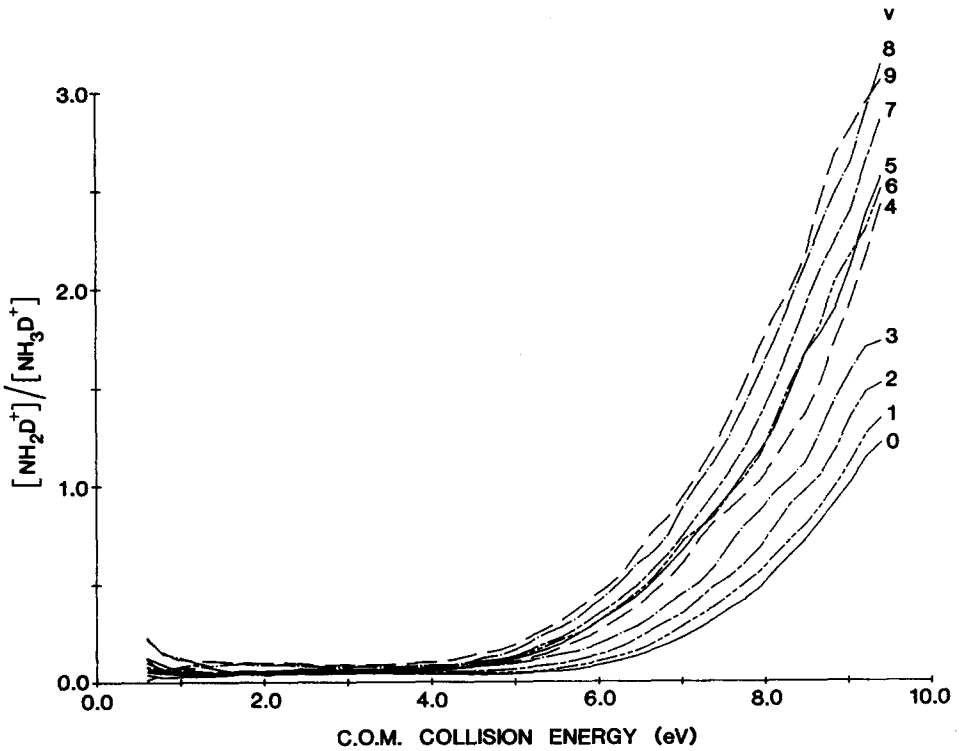

FIG. 6. Branching ratio plotted for $v = 0$ to $v = 9$ showing the increase in NH_2D^+ and decrease in NH_3D^+ as function of kinetic and ν_2 vibrational energy.

between the NH_2D^+ and the NH_3D^+ products. The full data set from $v = 0$ to $v = 9$ are plotted in this manner in Fig. 6. Plotting the data as a ratio of the two products eliminates the uncertainty associated with normalizing each data set to a constant primary ion flux. Additionally, this eliminates the instrumental biases that vary with the primary ion kinetic energy as discussed in the previous section, assuming that both product channels behave in a like manner. The amount of NH_2D^+ formed at low kinetic energies is less than 10% of the total product ion yield. At high kinetic energies, there is a clear shift in the onset of the NH_2D^+ channel with increasing vibrational excitation of the ν_2 mode of the NH_3^+. The addition of nine quanta of vibrational energy (1.1 eV) has the effect of shifting the branching ratio curve by nearly 2 eV to lower translational energy. This shift is in excess of the energy of the vibrational excitation of the NH_3^+ (v) ion.

IV. DISCUSSION

One of the goals of contemporary chemical dynamics is to determine those factors that influence the efficiency with which a particular molecular system reacts. Of prime importance is the examination of how the various forms of energy possessed by the reactant molecules (rotational, vibrational, electronic, and translational) are channeled into the products of a reaction. In this study, the NH_3^+ (v) + D_2 reaction has been examined as a function of ammonia ion translational and internal (the ν_2 umbrella-bending mode) energy. The results show that the NH_2D^+ and NH_3D^+ products observed at high kinetic energy are strongly related. The NH_2D^+ product increases beginning at 4–5 eV, implicating reaction (3) as the main source of the NH_2D^+ product at high kinetic energy. This is in agreement with the results of Eisele *et al.*,[13] who suggested that the NH_2D^+ is formed in a two-step process in which NH_3D^+ is created with excess internal excitation, leading to decomposition by the loss of an H atom. (Of course, the loss of the D atom is also possible, but the NH_3^+ product cannot be distinguished easily from the primary ion beam.) The initial vibrational excitation of the NH_3^+ is apparently an important contribution to the decomposition step. At first glance, this might suggest that excitation of the ν_2 mode plays some important dynamical role in the formation of NH_2D^+, but further considerations argue against this interpretation.

The internal energy deposited in the NH_3D^+ abstraction product can be calculated from a simple spectator-stripping model.[30] This model assumes that (1), the reaction proceeds in a direct manner, and (2), the internal energy of the NH_3^+ ion is completely retained in the NH_3D^+ product. The spectator-stripping model has been shown to be valid for a number of different systems at energies above 1 eV.[31,32] In the ideal limit, the incident NH_3^+ ion picks up one D atom while the other D atom acts as a spectator to the reaction. The spectator D atoms has the same velocity both before and after the collision so that there is no exchange of momentum with the incident ion. From the kinematic constraints of the model, the internal energy, W, of the NH_3D^+ product ion as a function of the NH_3^+ translational energy, E, and the vibrational energy, E_v, is given by

$$W = E \sin^2\beta + E_v - \Delta H, \tag{5}$$

where

$$\sin^2\beta \equiv [m(\mathrm{D})m(\mathrm{NH_3^+} + D_2)]/[m(\mathrm{NH_3D^+})m(D_2)]. \tag{6}$$

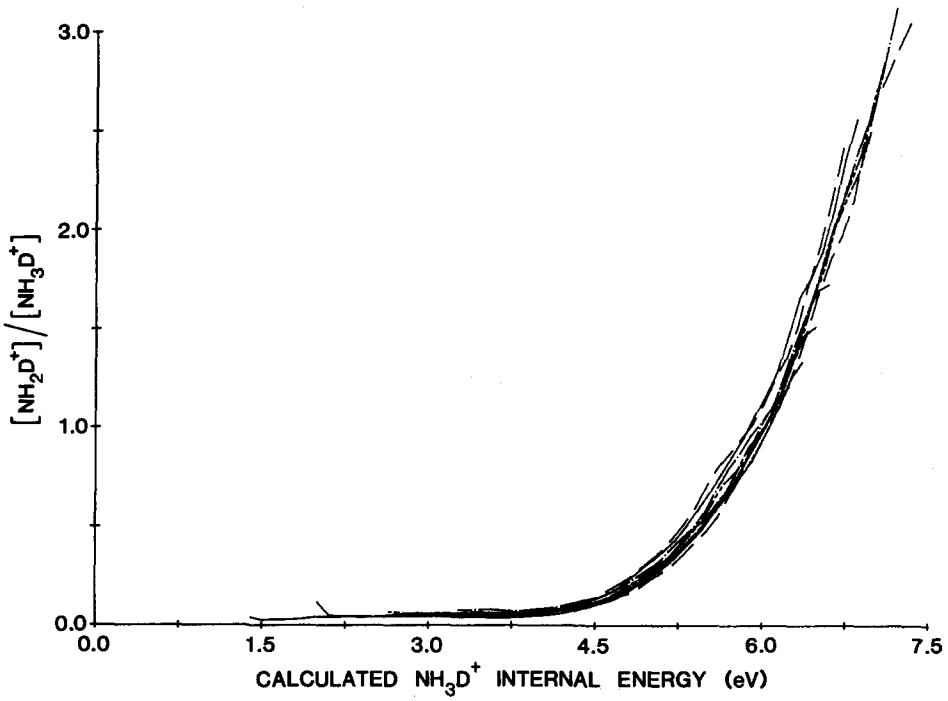

FIG. 7. Branching ratio as a function of the NH_3D^+ total internal energy as calculated from the classical spectator-stripping model [Eq. (5)] for the $v = 0$ to 9 data set.

For the $NH_3^+ + D_2$ system, $\sin^2\beta$ is 0.55 and ΔH is the reaction exothermicity of -1.04 eV. The data in Fig. 6 can be replotted as a function of the NH_3D^+ internal energy calculated from Eq. (5). The result, illustrated in Fig. 7, shows that the vibrational energy scales directly with the kinetic energy contribution of the $NH_3^+(v)$ ion to the NH_3D^+ total internal energy. The agreement of the data sets is sensitive to the fractional contribution of the NH_3^+ kinetic energy ($\sin^2\beta$) to within 0.55 ± 0.05. Thus, it appears that excitation of the ν_2 umbrella mode of the NH_3^+ need not play a dynamical role in the formation of NH_2D^+.

Karachevtsev *et al.*[19] also observed the NH_3D^+ production to peak at just over 4 eV in the center-of-mass, in agreement with this study. However, they did not give an account of the behavior or existence of the NH_2D^+ product. They reported that 1 eV internal excitation results in over a factor of 2 increase in the abstraction cross section at an energy of 0.5 eV. Because the ion signals in the present experiment decrease drastically below 1 eV, their observation could not be corroborated.

The tandem ICR experiments of Kemper and Bowers[20] were conducted at higher vibrational excitation and at much lower kinetic energy than can be reached in the present beam-gas experiment. They found that kinetic energy affected the abstraction rate much more than the exchange rate at 4 eV internal excitation. This is in agreement with an early activation barrier picture and is consistent with the data presented here. In addition, they found that vibrational energy affected the formation of NH_2D^+ much more than the formation of NH_3D^+ at thermal kinetic energies. If the NH_2D^+ that they observe is due strictly to molecular split-out [reaction (2)], then the large vibrational effect that they observed is not present at higher kinetic energies. On the other hand, if the NH_2D^+ is produced by decomposition [reaction (3)], then this confirms that vibration makes a direct energetic contribution to NH_3D^+ decomposition.

The classical spectator-stripping model gives a most probable value for the internal energy of the NH_3D^+ for a particular combination of NH_3^+ translational and vibrational energy. If the distribution of energies about this value were a delta function, then a step function would be observed at 5.5 eV in Fig. 7, corresponding to the difference in enthalpy between NH_3D^+ and $NH_2D^+ + D$. This assumes that the dissociative lifetime of the NH_3D^+ is much shorter than the microsecond time scale of the detection. Due to the spread in the incident ion kinetic energies and in the distribution introduced by the reactive collision itself, some of the NH_3D^+

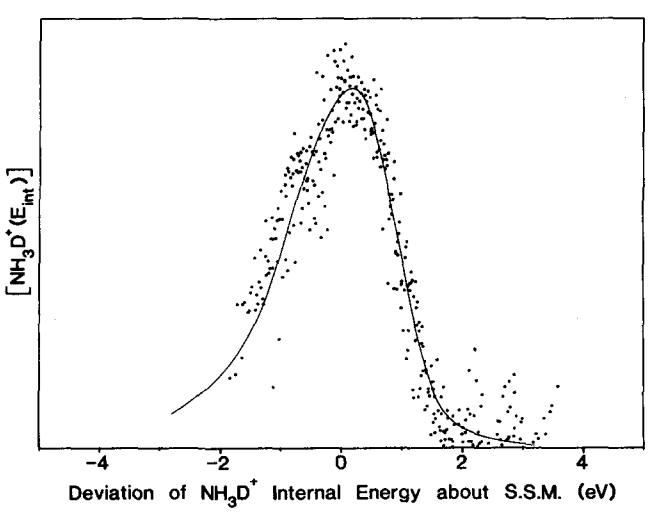

FIG. 8. The deconvolution of the $v = 0$ to 9 data sets to yield the distribution of the NH_3D^+ internal energy.

product ions will be formed with more or less internal energy than the model predicts. This distribution can be deconvoluted from the data curves in Fig. 7. At any particular energy, the fraction of ions appearing as NH_3D^+ is a measure of those ions having internal energies below the dissociation energy. Those that have internal energies above 5.5 eV decompose and are detected as NH_2D^+ (through loss of a H atom) or as NH_3^+ (through loss of a D atom). The NH_3D^+ internal energy distribution is the derivative of the fraction of ions appearing as NH_2D^+ (and phantom NH_3^+, assumed to be one-third of the NH_2D^+) out of the total ion yield.

Figure 8 shows the results of such an analysis showing the NH_3D^+ internal energy distribution relative to the energy predicted from the spectator-stripping model. The spectator-stripping model treats the reaction as a highly constrained system in which none of the energy is channeled into the spectator D atom. It is very unlikely that this is actually the case and one expects additional interaction between the species. A mathematically similar approach is to assume a pairwise interaction between the NH_3^+ and one of the D atoms in the laboratory reference frame, but without the kinematic constraints on the second deuterium. This allows the deuterium to interact in the abstraction mechanism and can result in a broad distribution of internal energy in the products.[33] A plausible intermediate for the hydrogen abstraction mechanism involves linear approach of the D_2 molecule along the C_3 axis of the ammonia ion

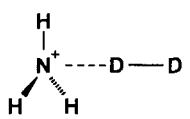

similar to that proposed by Bowers and co-workers for H abstraction in the NH_3^+/H_2O system.[34] The D_2 molecule can interact directly with the electron density on the nitrogen in this configuration. Other configurations such as the above but with the D_2 rotated by 90° or an in-plane approach appear less favorable. *Ab initio* and semiempirical calculations of portions of the NH_5^+ potential energy surface indicate that the above configuration represents a minimum energy approach and that the system must overcome a small barrier to form the highly stable NH_3D^+---D complex.[35–37]

Vibration in the ν_2 umbrella-bending mode is directed along the reaction coordinate in such a transition state. Increased vibration in this mode deforms the system towards the geometry of the tetrahedral product, which might suggest an increase in the total reaction cross section, but the experimental results show that the total reaction cross section is roughly independent of the ν_2 excitation. Whether steric hindrance from the hydrogens on the ammonia, the small mass of the spectator partner, or some other factor account for this behavior is presently a matter of conjecture.

V. CONCLUSIONS

We have successfully demonstrated the application of resonance-enhanced multiphoton ionization in the study of the ion–molecule reaction dynamics of NH_3^+. Multiphoton ionization is a highly specific technique for producing vibrationally state-selected ion beams. The ion intensity is sufficient to carry out studies on systems with low reactive cross sections such as NH_3^+/D_2.

Both NH_3D^+ and NH_2D^+ appear as products of the reaction of NH_3^+ with D_2. Hydrogen abstraction [reaction (1)] is the dominant reaction channel over the entire 0.5 to 10 eV kinetic energy range in the center-of-mass. Hydrogen–deuterium exchange by molecular split-out [reaction (2)] appears as only a very minor channel. Vibrational excitation of the ν_2 mode of the ammonia ion does not affect either reaction (1) or reaction (2) within the experimental uncertainty, but markedly affects the ratio of NH_2D^+ to NH_3D^+, as a result of reaction (3).

Formation of NH_2D^+ by the initial production of internally excited NH_3D^+ followed by the loss of atomic hydrogen [reaction (3)] becomes a significant pathway above a 4–5 eV onset. The initial vibrational excitation of the NH_3^+ (v) is an important contribution to the total internal energy deposited in the NH_3D^+ product ion and promotes the decomposition to form NH_2D^+. The energetic of this process are described quite well by a simple spectator-stripping model.

ACKNOWLEDGMENTS

The authors are grateful to David W. Chandler of Sandia National Laboratories (Livermore, CA) and Scott L. Anderson of the State University of New York (Stony Brook) for providing technical advice. We also wish to thank Michael T. Bowers and Peter B. Armentrout for helpful discussions. This work was supported by the Air Force Office of Scientific Research under Grant No. AFOSR F49620-85-C-0021.

[1] W. A. Chupka, M. E. Russell, and K. Refaey, J. Chem. Phys. **48**, 1518 (1968); W. A. Chupka and M. E. Russell, *ibid.* **48**, 1527 (1968).
[2] S. L. Anderson, F. A. Houle, D. Gerlich, and Y. T. Lee, J. Chem. Phys. **75**, 2153 (1981); T. Turner, O. Dutuit, and Y. T. Lee, *ibid.* **81**, 3475 (1984).
[3] T. Baer, in *Gas Phase Ion Chemistry*, edited by M. T. Bowers (Academic, New York, 1969), Chap. 5; T. R. Govers, P. M. Guyon, T. Baer, K. Cole, H. Fröhlich, and M. Lavollée, Chem. Phys. **87**, 373 (1984).
[4] K. Tanaka and I. Koyano, J. Chem. Phys. **69**, 3422 (1978); I. Koyano and K. Tanaka, *ibid.* **72**, 4858 (1980).
[5] P. R. Kemper, M. T. Bowers, D. C. Parent, G. Mauclaire, R. Derai, and R. Marx, J. Chem. Phys. **79**, 160 (1983); W. Wagner-Redeker, P. R. Kemper, M. T. Bowers, and K. R. Jennings, *ibid.* **80**, 3606 (1984).
[6] M. Durop-Ferguson, H. Böhringer, D. W. Fahey, and E. E. Ferguson, J. Chem. Phys. **79**, 265 (1983).
[7] R. J. S. Morrison, W. E. Conaway, and R. N. Zare, Chem. Phys. Lett. **113**, 435 (1985).
[8] J. T. Meek, S. R. Long, and J. P. Reilly, J. Phys. Chem. **86**, 2809 (1982); S. R. Long, J. T. Meek, and J. P. Reilly, J. Chem. Phys. **79**, 3206 (1983).
[9] S. L. Anderson, D. M. Rider, and R. N. Zare, Chem. Phys. Lett. **93**, 11 (1982); S. L. Anderson, G. D. Kubiak, and R. N. Zare, *ibid.* **105**, 22 (1984).
[10] S. T. Pratt, P. M. Dehmer, and J. L. Dehmer, J. Chem. Phys. **80**, 1706 (1984).
[11] A. Giardini-Guidoni and G. G. Volpi, Nuovo Cimento **17**, 919 (1960).
[12] A. G. Harrison and J. C. J. Thynne, Trans. Faraday Soc. **64**, 945 (1968).
[13] G. Eisele, A. Henglein, P. Botschwina, and W. Meyer, Ber. Bunsenges. Phys. Chem. **78**, 1090 (1974).
[14] J. K. Kim, L. P. Theard, and W. T. Huntress, Jr., J. Chem. Phys. **62**, 45 (1975).
[15] F. C. Fehsenfeld, W. Lindinger, A. L. Schmeltekopf, D. L. Albritton, and E. E. Ferguson, J. Chem. Phys. **62**, 2001 (1975).
[16] N. G. Adams, D. Smith, and J. F. Paulson, J. Chem. Phys. **72**, 288 (1980); N. G. Adams and D. Smith, Int. J. Mass Spectrom. Ion Phys. **61**, 113 (1984).
[17] J. A. Luine, Ph.D. thesis, University of Colorado, Boulder, 1981.

[18]S. E. Barlow, Ph.D. thesis, University of Colorado, Boulder, 1984.
[19]G. V. Karachevtsev, V. M. Matyuk, V. K. Potapov, and A. A. Prokof'ev, Khim. Vys. Energ. **14**, 81 (1980).
[20]P. R. Kemper and M. T. Bowers, Chem. Phys. (submitted).
[21]R. A. Yost and D. D. Fetteroff, Mass Spectrom. Rev. **2**, 1 (1983).
[22]J. H. Glownia, S. J. Riley, S. D. Colson, and G. C. Nieman, J. Chem. Phys. **72**, 5998 (1980); *ibid.* **73**, 4296 (1980).
[23]J. H. Glownia, S. J. Riley, S. D. Colson, J. C. Miller, and R. N. Compton, J. Chem. Phys. **77**, 68 (1982).
[24]M. N. R. Ashford, R. N. Dixon, and R. J. Strickland, Chem. Phys. **88**, 463 (1984).
[25]A. J. Grimley and B. D. Kay, Chem. Phys. Lett. **98**, 359 (1983).
[26]R. J. Stanley, O. Echt, and A. W. Castleman, Jr., Appl. Phys. Lett. B **32**, 35 (1983).
[27]Y. Achiba, K. Sato, K. Shobatake, and K. Kimura, J. Chem. Phys. **78**, 5474 (1983).
[28]W. E. Conaway, R. J. Morrison, and R. N. Zare, Chem. Phys. Lett. **113**, 429 (1985).
[29]B. D. Kay and T. D. Raymonds (unpublished work).
[30]A. Henglein, K. Lacmann, and G. Jacobs, Ber. Bunsenges. Phys. Chem. **69**, 286 (1965); A. Henglein, in *Ion–Molecule Reactions in the Gas Phase*, edited by P. J. Ausloos (American Chemical Society, Washington, D. C., 1966), Chap. 5.
[31]J. R. Wyatt, L. W. Stratton, S. C. Snyder, and P. M. Hierl, J. Chem. Phys. **62**, 2555 (1975).
[32]S. A. Safron, in *Specialist Periodical Reports*: *Mass Spectrometry Vol. 7* (Royal Society of Chemistry, London, 1984), Chap. 3.
[33]P. B. Armentrout (private communication).
[34]M. T. Bowers and T. Su, Adv. Electron. Electron Phys. **34**, 257 (1973); W. J. Chesnavich and M. T. Bowers, Chem. Phys. Lett. **52**, 179 (1977).
[35]O. P. Bugaets and D. A. Zhogolev, Chem. Phys. Lett. **45**, 462 (1977).
[36]G. V. Karachevtsev, A. Z. Marutkin, V. L. Tal'roze, and S. P. Tachenko, Kim. Vys. Energ. **13**, 11 (1979).
[37]P. von R. Schleyer (private communication).